LA-8799-MS

c.3

Nuclear Accident Dosimetry: Los Alamos Measurements at the Seventeenth Nuclear Accident Dosimetry Intercomparison Study at the Oak Ridge National Laboratory DOSAR Facility, August 1980

LOS ALAMOS SCIENTIFIC LABORATORY
Post Office Box 1663 Los Alamos, New Mexico 87545

This report was not edited by the Technical Information staff.

UNITED STATES
DEPARTMENT OF ENERGY
CONTRACT W-7405-ENG. 36

LA-8799-MS
UC-41
Issued: April 1981

Nuclear Accident Dosimetry: Los Alamos Measurements at the Seventeenth Nuclear Accident Dosimetry Intercomparison Study at the Oak Ridge National Laboratory DOSAR Facility, August 1980

Dennis G. Vasilik
Robert W. Martin

NUCLEAR ACCIDENT DOSIMETRY: LOS ALAMOS MEASUREMENTS AT THE SEVENTEENTH NUCLEAR ACCIDENT DOSIMETRY INTERCOMPARISON STUDY AT THE OAK RIDGE NATIONAL LABORATORY DOSAR FACILITY, AUGUST 1980

by

Dennis G. Vasilik
Robert W. Martin

ABSTRACT

Teams from various US and foreign organizations participated in the Seventeenth Nuclear Accident Dosimetry Study held at the Oak Ridge National Laboratory's (ORNL) Dosimetry Applications Research (DOSAR) facility August 11-15, 1980. Criticality dosimeters were simultaneously exposed to pulses of mixed neutron and gamma radiation from the Health Physics Research Reactor (HPRR). This report summarizes the experimental work conducted by the Los Alamos team. ORNL will publish a report comparing the results of all participants who made similar measurements under identical conditions. In-air and phantom measurements were conducted by the Los Alamos team using area and personnel dosimeters. Combined blood sodium and sulfur fluence measurements of absorbed dose were also made. In addition, indium foils placed on phantoms were evaluated for the purpose of screening personnel for radiation exposure. All measurements were conducted for unshielded, 5-cm steel and 20-cm concrete shielding configurations. All participant dosimeters were exposed at 3 m from the center of the HPRR core.

I. INTRODUCTION

This report presents the final results of the Los Alamos measurements. Included are those results provided to DOSAR in a form amenable to comparison with other participants. Also included are the results of additional studies and evaluations conducted by Los Alamos at Oak Ridge.

The Seventeenth Nuclear Accident Dosimetry (NAD) Intercomparison Study was held at the Oak Ridge National Laboratory's DOSAR facility August 11-15, 1980. The intercomparison study consisted of the simultaneous exposure of the participants' dosimeters to pulsed radiation from the HPRR reactor.[1-5]

Los Alamos had participated in previous intercomparison studies at the Oak Ridge National Laboratory.[6] The present NAD study provided an opportunity to expose criticality dosimeters to different degraded neutron energy spectra. These studies provide a valuable opportunity to evaluate Los Alamos concepts of criticality dosimetry and to direct future lines of endeavor.

II. EXPERIMENTAL DESCRIPTION

The HPRR served as a source of pulsed radiation. Three typical nuclear accident spectra were simulated by operating the reactor (a) unshielded, (b) shielded by 5-cm of steel, and (c) shielded by 20-cm of concrete. At this NAD study, all measurements were conducted at 3-m from the center of the HPRR core. The shields were located 1-m from the HPRR core. Three phantoms were located with their mid-points at 3-m from the center of the HPRR core. One phantom (A) was filled with a saline solution and its front faced the reactor core. Another phantom (B) was filled with a saline solution and its side faced the reactor core. Phantoms A and B had nominal saline concentrations of 1.55 mg sodium per ml of water. A third phantom (C) was filled with water and its front faced the core. It was not used for the Los Alamos studies.

Table I shows the data related to the three pulses from the HPRR during this intercomparison. The neutron doses provided by ORNL are based on measured sulfur tablet activations and known shield attenuation factors.[7]

TABLE I

PULSE DATA FOR 17TH NAD STUDY

Pulse	Date	Time (EDT)	Fissions	Shield	Neutron Dose (rad)
1	8/12/80	10:36 a.m.	7.61×10^{16}	None	290
2	8/13/80	11:20 a.m.	4.54×10^{16}	5-cm steel	112
3	8/14/80	11:12 a.m.	5.18×10^{16}	20-cm concrete	52

III. DOSIMETRY

A. Personnel Dosimeters

A Personnel Neutron Dosimeter (PND) packet is used to estimate the neutron dose to a person carrying the device. PND packets are issued to persons working in all Los Alamos areas where a nuclear accident is possible. PND packets were placed on the front and back of phantom A for each HPRR pulse. The elements of the PND system are given in Table II. Figure 1 is a line drawing of the PND packet.

Neutron activation analysis is used to determine the fluence of a neutron spectrum.[8]

TABLE II

COMPONENTS OF PND PACKET

Dosimeter	Neutron Energy Range
Bare indium foil	0.025 - 0.5 eV
Cadmium covered indium foil	0.5 - 2.0 eV and 1 - 9 MeV
Cadmium covered copper foil	10^{-5} - 1 MeV
Sulfur tablet	2.9 - 9 MeV

B. Area Dosimeters

The Los Alamos Criticality Dosimeter (LACD) packet is an area monitor located wherever a potential exists for a nuclear accident.

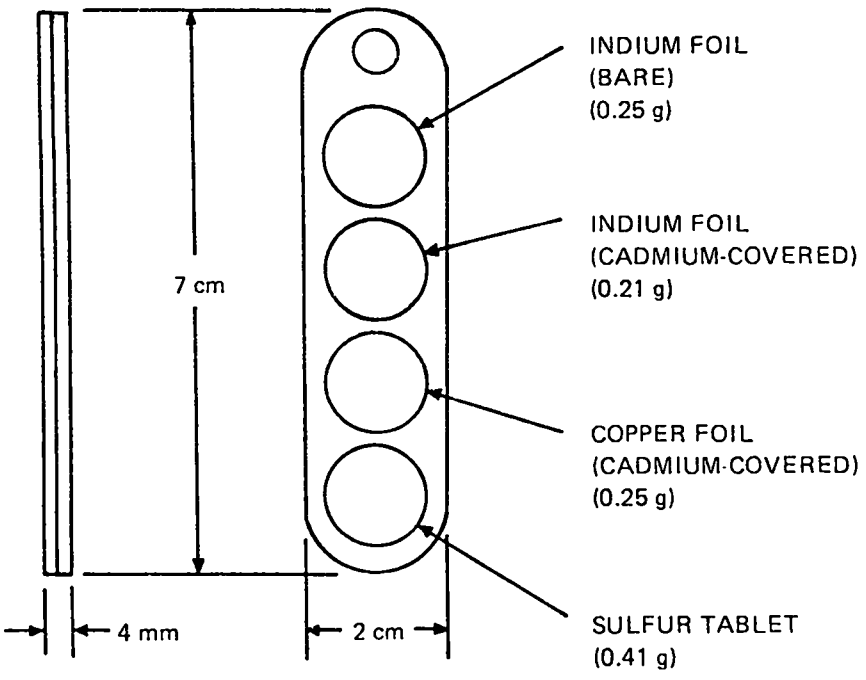

Fig. 1.
Personnel Neutron Dosimeter (PND) packet.

The elements of the LACD packet are given in Table III. Figure 2 is a line drawing of the LACD packet. The LACD packet is capable of providing neutron and photon dose estimates. Activation foils are used to determine the neutron dose. Photon doses are measured with thermoluminescent dosimeters (TLD-700) and silver-activated phosphate glass rods. The LACD packet is described in detail in the literature.[8] LACD packets were used to measure the in-air doses for each of the three HPRR pulses.

C. Body Sodium Analysis

The determination of the dose that an individual receives in a criticality accident can be very difficult. In general, one requires a knowledge of the general shape of the neutron energy spectrum incident on the body. If the spectral shape can be estimated, then systems such as the LACD and PND packets can be used to provide accurate dose estimates[8] per suggested IAEA guidelines.[9] IAEA suggests an accuracy of 50% in the dose determination in 24 hours and 25% in four days. If the spectral shape cannot be estimated, then great

TABLE III

COMPONENTS OF LACD PACKET

Dosimeter	Energy Range
Bare indium foil	0.025 - 0.5 eV
Cadmium covered indium foil	0.5 - 2.0 eV and 1 - 9 MeV
Bare gold foil	0.025 - 0.5 eV
Cadmium covered gold foil	0.5 - 10.0 eV
Cadmium covered copper foil	10^{-5} - 1 MeV
Sulfur tablet	2.9 - 9 MeV
Phylatron diode	0.4 - 9 MeV
Thermoluminescent dosimeters (TLD-700)	0.005 - 15 MeV
Glass rod dosimeter	0.005 - 15 MeV

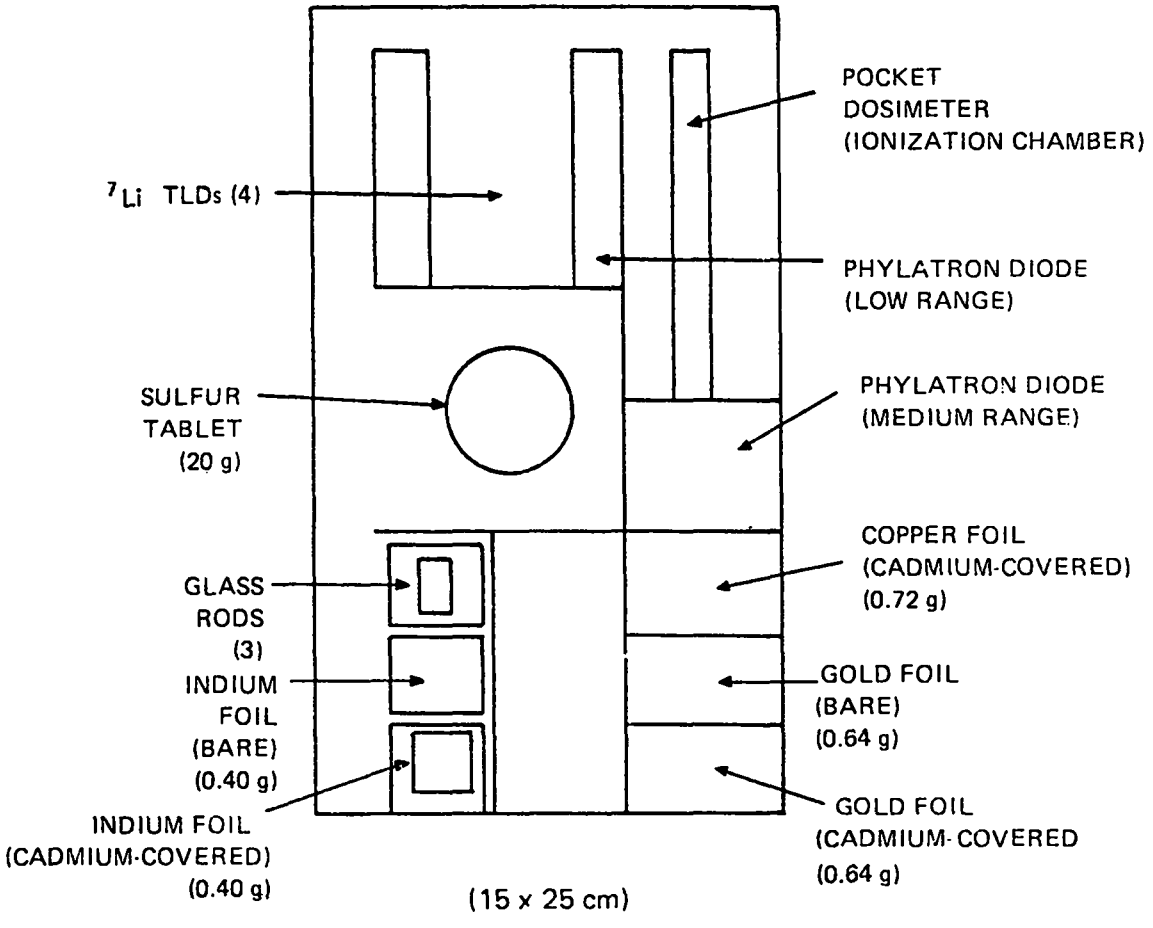

Fig. 2.
Los Alamos Criticality Dosimetry (LACD) packet.

difficulties can prevail in the determination of the dose. Factors that affect the activation of threshold foils include the configuration of the source material, whether or not shielding is between the source and the individual, where the individual was located with respect to floors, walls, and equipment, and the orientation of the individual. It is also possible that an individual might not have worn a dosimeter, or an area dosimeter might not be retrievable.

The Laboratory also uses an additional technique to determine the neutron dose which depends on a combination of blood- and hair-activation. Blood-sodium activation is a well known technique for determining the dose from a criticality accident.[10] The activation of hair sulfur is also a well known technique for determining the neutron dose.[11,12,13] Hankins has shown[14] that the ratio of sulfur fluence to blood sodium activation as a function of blood sodium activation can result in dose estimates that are accurate to within ± 20-30%. This technique is independent of the neutron energy spectrum, individual orientation, neutron scattering, and shielding (except for massive metal shields). In combination with the results of PND and/or LACD dosimetry, this technique can provide accurate dose assessments of a potential criticality accident. For these experiments, sulfur tablets were used to determine the sulfur fluences. Hair also can provide a good estimate of the sulfur fluence. Hair would be used in the case of an exposed individual who did not wear a dosimeter which included sulfur.

D. Personnel Dosimeter Screening

Early screening of potentially exposed individuals can be accomplished by determining the activity of the indium foils in a PND packet with a Geiger-Müller instrument. The measured dose-rate from the indium in mR/hr (corrected for decay time since exposure) can be related to the neutron dose with appropriate calibration factors. Indium activation studies have been conducted for a large number of critical assemblies.[10] If a critical excursion is similar to one occurring in assemblies studied, the neutron dose could be estimated to within ± 50%. Any indium activation is usually a sign that an individual involved in a criticality accident has been exposed to neutrons. Screening could be a valuable tool for determining response priorities in a criticality accident.

IV. RESULTS

A. Neutron Dosimetry

Table IV shows the threshold detectors that are used in the PND and LACD packets. The particular reactions of interest and the applicable energy ranges for fluence determinations are shown. The threshold detectors are treated as if they were ideal detectors with defined thresholds, E_{th}, and with only one cross-section, $\bar{\sigma}$. If one knows the shape of the neutron energy spectrum, then the effective cross section, $\bar{\sigma}$, for the detector is defined by:

$$\bar{\sigma} = \frac{\int_{E_o}^{\infty} \frac{dN}{dE}(E)\sigma(E)dE}{\int_{E_{th}}^{\infty} \frac{dN}{dE}(E)dE}$$

where

$\bar{\sigma}$ = the effective cross section for the detector,

$\frac{dN}{dE}(E)$ = the irradiating neutron energy spectrum,

$\sigma(E)$ = the detector cross section,

E_o = the absolute threshold energy for the detector,

E_{th} = the effective threshold energy that one chooses for the detector.

TABLE IV

PND AND LACD DOSIMETER THRESHOLD FOILS

Number	Foil Type	Packet Location(s)	Energy Range	Nuclear Reaction of Interest
1.	Cadmium Covered Indium	PND and LACD	1 - 9 MeV	$^{115}_{49}In + ^{1}_{0}n \rightarrow ^{115m}_{49}In + ^{1}_{0}n'$
2.	Sulfur Tablet	PND and LACD	2.9 - 9 MeV	$^{32}_{16}S + ^{1}_{0}n \rightarrow ^{32}_{15}P + ^{1}_{1}P$ $^{32}_{15}P \xrightarrow[\beta -]{} ^{32}_{16}S$
3.	Cadmium Covered Copper	PND and LACD	10^{-5} - 1 MeV	$^{63}_{29}Cu + ^{1}_{0}n \rightarrow \left(^{64}_{29}Cu\right)^{*} \xrightarrow[\beta+]{} ^{64}_{28}Ni + \gamma's$
4.	Bare Indium Cadmium Covered Indium	PND and LACD	Thermal and Epithermal	$^{115}_{49}In + ^{1}_{0}n \rightarrow \left(^{116m}_{49}In\right)^{*} \xrightarrow[\beta-]{} ^{116}_{50}Sn + \gamma's$
5.	Bare Gold Cadmium Covered Gold	LACD	Thermal and Epithermal	$^{197}_{79}Au + ^{1}_{0}n \rightarrow \left(^{198}_{79}Au\right)^{*} \xrightarrow[\beta-]{} ^{198}_{80}Hg + \gamma's$

For this intercomparison study, appropriate neutron energy spectra for HPRR were available[15,16] to determine the effective cross sections for each burst. The neutron fluence, ϕ, in each energy interval is determined from the activation produced in each foil along with the appropriate effective cross sections.[8]

The neutron dose determination (absorbed dose, first collision dose, or Kerma dose in tissue) is made by multiplying the fluence in each energy region by the appropriate fluence-to-dose conversion factor and summing the individual doses. The uncertainty associated with a measurement of a neutron dose will be directly proportional to the uncertainties associated with the effective cross sections.

In Figure 3 we show:

1. Absorbed dose [17] for a homogeneous anthropomorphic phantom which is a right circular cylinder with a radius r = 15-cm and a height h = 60-cm. The phantom is composed of H, C, N, and O in the proportions of standard man.[18] The absorbed dose is for Element 57 of the phantom.
2. First collision dose [18] for soft tissue.
3. Kerma dose[19] for soft tissue.

Absorbed dose and first collision dose must have the units of rads whereas tissue Kerma dose is always reported as $erg \cdot g^{-1}$. Appropriate fluence-to-dose

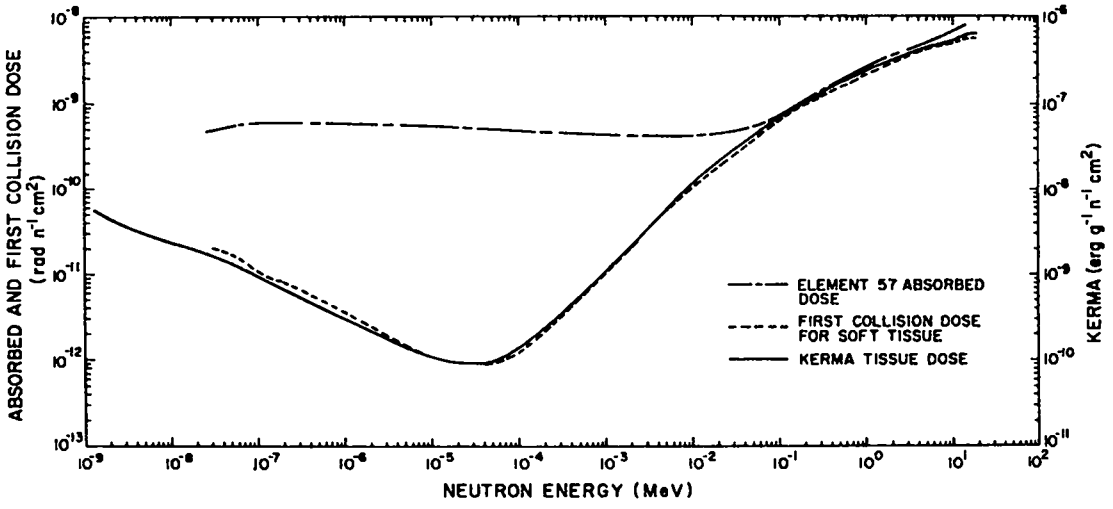

Fig. 3.

Variation of dose with neutron energy.

conversion factors used in this report were determined by a weighting technique described by:

$$\overline{DF} = \frac{\int_{E_1}^{E_2} \frac{dN}{dE}(E)DF(E)dE}{\int_{E_1}^{E_2} \frac{dN}{dE}(E)dE} \qquad (1)$$

where,

DF(E) = Appropriate fluence-to-dose conversion factor as a function of energy.

$\frac{dN}{dE}(E)$ = Irradiating neutron energy spectrum (n/cm^2-MeV).

$\overline{DF}$ = Effective fluence-to-dose conversion factor for the neutron energy range from E_1 to E_2.

1. LACD Results. A summary of the LACD area dosimeter results is given in Table V for each HPRR burst. Neutron fluences for the appropriate energy ranges are presented. In addition, we show the tissue Kerma dose, Element 57 neutron dose, and photon dose. The Element 57 dose is partitioned according to the relative contributions due to the $^1H(n,\gamma)^2H$ reaction and charged particle reactions (recoils plus protons).[17]

In Table VI we show the absorbed neutron dose (Element 57) to photon dose ratio for each pulse. Our measured values are compared to reported Oak Ridge values.[6]

In Table VII we show the effective cross sections used for the components of the LACD for burst number one. Also shown are the reaction rates (equal to $\phi\sigma \times 10^{10}$) corrected to time of burst per 10^{10} atoms, for each activation foil. Tables VIII and IX show these data for burst numbers two and three, respectively.

2. PND Results. PND packets were placed on the chest and back of phantom A for each HPRR burst. The PND packet on the front of the phantom was used to determine tissue Kerma dose and Element 57 absorbed dose. The activation data for the PNDs on the phantom chest were corrected for neutron backscatter. In Table X we show the PND packet results on the phantom chest for each burst. The

TABLE V

ORNL SEVENTEENTH INTERCOMPARISON OF NUCLEAR ACCIDENT DOSIMETERS
IN AIR STUDIES WITH LACD DOSIMETER

	NEUTRON FLUENCE ($n \cdot cm^{-2} \times 10^{10}$)								Tissue Kerma Dose ($herg \cdot g^{-1}$)	Element 57 Neutron Dose (rad)		Photon Dose (rad)
Pulse Number	Foil Cover Energy	Gold Bare Thermal	Gold Cadmium Epithermal	Indium Bare Thermal	Indium Cadmium Epithermal	Copper Cadmium 10^{-5}–1 MeV	Indium Cadmium 1–9 MeV	Sulfur Bare 2.9–9 MeV		Recoils Plus Protons	$^1H(n,\gamma)^2H$	
1		0.83	0.066	1.47	0.062	8.70	4.60	2.35	291	262	24.3	45.0
2		0.37	0.033	0.63	0.031	5.97	1.74	0.28	125	108	14.1	18.5
3		1.54	0.060	0.98	0.060	0.63	0.74	0.31	37.9	33.7	6.76	21.5

TABLE VI

ABSORBED NEUTRON DOSE TO PHOTON DOSE
RATIOS FOR IN-AIR LACD DOSIMETER MEASUREMENTS

Pulse Number	Dn/Dγ Ratio (Measured)	Dn/Dγ Ratio (Expected)*
1	6.4	6.2 ± 0.8
2	6.6	–
3	1.9	2.2 ± 0.8

*Reference 6.

TABLE VII

BURST NUMBER 1: LACD COMPONENT
EFFECTIVE CROSS SECTIONS AND REACTION RATES PER 10^{10} ATOMS

Detector Component	Effective Cross Section (Cm^2)	Energy Range	Reaction Rate Per 10^{10} Atoms ($\phi\sigma \times 10^{10}$)
Bare Gold	1.07×10^{-22}	Thermal	8.91×10^{-3}
Cadmium Covered Gold	1.55×10^{-21}	Epi-Thermal 0.62–10 eV	1.02×10^{-2}
Bare Indium	1.96×10^{-22}	Thermal	2.88×10^{-2}
Cadmium Covered Indium (n,γ)	2.60×10^{-21}	Epi-Thermal 0.62–2 eV	1.60×10^{-2}
Cadmium Covered Copper	1.06×10^{-25}	10^{-5}–1 MeV	9.22×10^{-5}
Cadmium Covered Indium (n,n')	2.24×10^{-25}	1–9 MeV	1.03×10^{-4}
Sulfur	1.60×10^{-25}	2.9–9 MeV	3.76×10^{-5}

TABLE VIII

BURST NUMBER 2: LACD COMPONENT
EFFECTIVE CROSS SECTIONS AND REACTION RATES PER 10^{10} ATOMS

Detector Component	Effective Cross Section (Cm^2)	Energy Range	Reaction Rate Per 10^{10} Atoms ($\phi\sigma \times 10^{10}$)
Bare Gold	1.07×10^{-22}	Thermal	3.97×10^{-3}
Cadmium Covered Gold	1.55×10^{-21}	Epi-Thermal 0.62-10 eV	5.12×10^{-3}
Bare Indium	1.96×10^{-22}	Thermal	1.23×10^{-2}
Cadmium Covered Indium (n,γ)	2.60×10^{-21}	Epi-Thermal 0.62-2 eV	7.93×10^{-3}
Cadmium Covered Copper	8.90×10^{-26}	10^{-5}-1 MeV	5.31×10^{-5}
Cadmium Covered Indium (n,n')	2.28×10^{-25}	1-9 MeV	3.97×10^{-5}
Sulfur	2.76×10^{-25}	2.9-9 MeV	7.67×10^{-6}

TABLE IX

BURST NUMBER 3: LACD COMPONENT
EFFECTIVE CROSS SECTIONS AND REACTION RATES PER 10^{10} ATOMS

Detector Component	Effective Cross Section (Cm^2)	Energy Range	Reaction Rate Per 10^{10} Atoms ($\phi\sigma \times 10^{10}$)
Bare Gold	1.07×10^{-22}	Thermal	1.65×10^{-2}
Cadmium Covered Gold	1.55×10^{-21}	Epi-Thermal 0.62-10 eV	9.05×10^{-3}
Bare Indium	1.96×10^{-22}	Thermal	1.93×10^{-2}
Cadmium Covered Indium (n,γ)	2.60×10^{-21}	Epi-Thermal 0.62-2 eV	1.63×10^{-2}
Cadmium Covered Copper	5.65×10^{-25}	10^{-5}-1 MeV	5.14×10^{-6}
Cadmium Covered Indium (n,n')	2.43×10^{-25}	1-9 MeV	1.79×10^{-5}
Sulfur	2.35×10^{-25}	2.9-9 MeV	7.19×10^{-6}

TABLE X

ORNL SEVENTEENTH INTERCOMPARISON OF NUCLEAR ACCIDENT DOSIMETERS
PND PACKETS ON CHEST OF PHANTOM A

Pulse Number	Tissue Kerma Dose ($herg \cdot g^{-1}$)	Element 57 Neutron Dose (rad)		Photon Dose (rad)
		Recoils Plus Protons	$^1H(n,\gamma)^2H$	
1	318	274	30.4	45
2	135	125	15.8	18.5
3	32	25.4	5.6	21.5

TABLE XI

BURST NUMBER 1: PND COMPONENT
EFFECTIVE CROSS SECTIONS AND REACTION RATES
PER 10^{10} ATOMS
CHEST PHANTOM A

Detector Component	Effective Cross Section (cm^2)	Energy Range	Reaction Rate Per 10^{10} Atoms ($\phi\sigma \times 10^{10}$)
Indium (Bare)	1.96×10^{-22}	Thermal	4.17×10^{-2}
Cadmium Covered Indium (n, γ)	2.60×10^{-21}	Epi-Thermal 0.62 - 2 eV	5.12×10^{-2}
Cadmium Covered Copper	1.06×10^{-25}	10^{-5}-1 MeV	8.59×10^{-5}
Cadmium Covered Indium (n, n')	2.24×10^{-25}	1-9 MeV	9.83×10^{-5}
Sulfur	1.60×10^{-25}	2.9-9 MeV	2.59×10^{-5}

Element 57 dose is partitioned according to the relative contributions due to the $^1H(n,\gamma)^2H$ reaction and charged particle reactions.

In Table XI we show the effective cross sections used for the components of the PND on the chest of phantom A for burst number one. Also shown are the reaction rates (equal to $\phi\sigma \times 10^{10}$) corrected to time of burst per 10^{10} atoms, for each activation foil. Tables XII and XIII show these data for burst numbers two and three, respectively.

TABLE XII

BURST NUMBER 2: PND COMPONENT
EFFECTIVE CROSS SECTIONS AND REACTION RATES
PER 10^{10} ATOMS
CHEST PHANTOM A

Detector Component	Effective Cross Section (cm^2)	Energy Range	Reaction Rate Per 10^{10} Atoms ($\phi\sigma \times 10^{10}$)
Indium (Bare)	1.96×10^{-22}	Thermal	1.93×10^{-2}
Cadmium Covered Indium (n, γ)	2.60×10^{-21}	Epi-Thermal 0.62 - 2 eV	2.17×10^{-2}
Cadmium Covered Copper	8.90×10^{-26}	10^{-5}-1 MeV	4.66×10^{-5}
Cadmium Covered Indium (n, n')	2.28×10^{-25}	1-9 MeV	5.55×10^{-5}
Sulfur	2.76×10^{-25}	2.9-9 MeV	1.37×10^{-5}

TABLE XIII

BURST NUMBER 3: PND COMPONENT
EFFECTIVE CROSS SECTIONS AND REACTION RATES
PER 10^{10} ATOMS
CHEST PHANTOM A

Detector Component	Effective Cross Section (cm^2)	Energy Range	Reaction Rate Per 10^{10} Atoms ($\phi\sigma \times 10^{10}$)
Indium (Bare)	1.96×10^{-22}	Thermal	2.14×10^{-2}
Cadmium Covered Indium (n, γ)	2.60×10^{-21}	Epi-Thermal 0.62 - 2 eV	2.56×10^{-2}
Cadmium Covered Copper	5.65×10^{-25}	10^{-5}-1 MeV	5.82×10^{-5}
Cadmium Covered Indium (n, n')	2.43×10^{-25}	1-9 MeV	7.02×10^{-6}
Sulfur	2.35×10^{-25}	2.9-9 MeV	6.79×10^{-6}

In Table XIV we summarize the results for PND packets placed on the chest and back of phantom A for each burst. In Table XV we show the ratio of the doses measured at the rear of the phantom to the doses at the front of the phantom for each burst. No corrections due to the presence of the phantoms were applied to PND data for the dosimeters placed on the back of the phantoms.

3. Body Sodium Analysis. Los Alamos blood-sodium analyses were conducted on phantoms A and B for each HPRR burst. A summary of the blood-sodium analyses is presented in Table XVI.

In Table XVII we show a comparison of blood-sodium dose estimates with in-air (LACD) absorbed dose determinations. Also shown is the ratio of LACD and Phantom A chest (PND) absorbed dose measurements for each burst. Finally, we show in this table ORNL data[6] for the ratio of measured dose in air to the dose measured on a phantom.

4. Personnel Dosimeter Screening Analysis. For each HPRR burst, PND packets were placed on the chest and back of phantom A for the purpose of evaluating indium activation for personnel exposure screening. A PND was also placed on the front chest of phantom B (the side of phantom B was facing the HPRR core). In Table XVIII we summarize the results of the Geiger counter readings of the indium foil in the PND packet. All these data were acquired with a LUDLUM 14C G-M meter, with a closed shield, in contact with the indium foil. All readings are corrected to the time of burst. All foils decayed with a 54 min half-life characteristic of ^{116m}In decay. The G-M dose-rate to rad neutron ratios are based on the LACD Element 57 dosimetry results of Table V.

TABLE XIV

SUMMARY OF PND RESULTS FOR ORNL HPRR EXPERIMENTS

Burst Number	PND Position on Phantom A	Absorbed Neutron Dose (rad)	Thermal Neutron Dose (rad)	Neutron Fluence x 10^{-10} (n/cm^2)		
				Cu	In	S
1	Chest	304	7.6	8.10	6.01	1.62
	Back	95.5	5.9	5.02	0.79	0.48
2	Chest	141	3.3	5.24	2.44	0.50
	Back	41.4	0.1	0.44	1.28	0.06
3	Chest	31	3.6	1.03	0.36	0.29
	Back	7.5	0.4	0.32	0.08	0.05

TABLE XV

RATIO OF PND ABSORBED NEUTRON DOSES
FROM REAR TO FRONT OF PHANTOM A AT 3 METERS FROM HPRR CORE

Burst Number	Configuration	$Dose_n$ Rear/$Dose_n$ Front
1	Unshielded	0.31
2	5-cm Steel	0.29
3	20-cm Concrete	0.24

TABLE XVI

ORNL SEVENTEENTH INTERCOMPARISON STUDY
BLOOD SODIUM ANALYSIS RESULTS

Burst Number	Phantom Designation	Na_{24} Activity (μCi ^{24}Na/mg ^{23}Na)	Sulfur Fluence to Sodium Activation (n/cm^2) Per (μCi ^{24}Na/mg ^{23}Na)	Neutron Absorbed Dose Estimate (rad)
1	A	6.83×10^{-4}	3.29×10^{13}	285
	B	4.53×10^{-4}	5.19×10^{13}	283
2	A	3.61×10^{-4}	7.70×10^{12}	103
	B	2.14×10^{-4}	1.30×10^{13}	96.4
3	A	1.63×10^{-4}	1.88×10^{13}	49.4
	B	9.95×10^{-5}	3.08×10^{13}	53.8

TABLE XVII

COMPARISON BLOOD SODIUM DOSE ESTIMATES WITH LACD
AND PND DOSE DETERMINATIONS

Burst Number	Configuration	Ratio of LACD Dose To Blood-Sodium Dose (Absorbed)	Ratio of LACD Absorbed Dose to PND Absorbed Dose Measured on Chest of Phantom A	ORNL Ratio[6] of Measured in Air to Dose Measured on Phantom
1	Unshielded	0.99	0.94	0.96 ± 0.09
2	5-cm Steel	0.82	0.87	–
3	20-cm Concrete	1.28	1.31	0.83 ± 0.52

TABLE XVIII

SUMMARY OF GEIGER COUNTER ANALYSES
INDIUM FOILS IN PND DOSIMETER
(AVERAGE WEIGHT OF BARE INDIUM FOIL IN PNDs IS 0.236 g)

Burst Number	Configuration	PND Location on Phantom	Geiger Counter Dose-Rate* Per rad Neutron (mR/hr-radn)	Dose-Rate Per rad Neutron at Each Location/Dose-Rate Per rad Neutron at Front of Phantom
1	Unshielded	Front	5.69×10^{-1}	1.00
	Unshielded	Back	6.99×10^{-2}	0.12
	Unshielded	"Side"	2.51×10^{-1}	0.44
2	5-cm Steel	Front	9.34×10^{-1}	1.00
	5-cm Steel	Back	1.28×10^{-1}	0.14
	5-cm Steel	"Side"	5.57×10^{-1}	0.60
3	20-cm Concrete	Front	2.25×10^{0}	1.00
	20-cm Concrete	Back	2.96×10^{-1}	0.13
	20-cm Concrete	"Side"	7.90×10^{-1}	0.35

*Corrected to the time of burst.

B. Photon Dosimetry

Thermoluminescent Dosimeters. Photon dose is measured primarily with thermoluminescent dosimeters (TLD). Only the LACD dosimeter includes the TLD devices. Harshaw TLD-700 LiF chips (0.318 cm x 0.318 cm x 0.089 cm) are used. The TLD-700 dosimeters contain 0.007% Li-6 and 99.993% Li-7. The TLD-700 has a very low neutron sensitivity.[10]. Four TLD-700 dosimeters are located inside of a plastic disk for protective purposes. Photon doses can be measured from 25 millirads to about 10^4 rads with an accuracy of 10%. Standard calibration curves are used to relate photon dose to the light units determined with a TLD reader.

The photon dosimetric results for this NAD study have been included in the previous Neutron Dosimetry Section for ease of compilation.

V. DISCUSSION

These studies have demonstrated some of the capabilities and advantages of the methods used at Los Alamos for criticality dosimetry. None of the systems described rely on elaborate computational or experimental programs.[8] The systems, for these experiments, satisfy the suggested requirements[9] of a criticality accident dosimetry program which provides estimates of the dose within an accuracy of 50% in 24 hours and 25% within four days.

The NAD study provided an excellent opportunity to evaluate our methods for determining effective cross sections.[8] The study also strongly supported the procedures suggested by Hankins[14] for the dosimetry of criticality accidents using activations of blood and sulfur (hair or tablets).

As of this writing, the final NAD intercomparison report has not been published. However, preliminary results from Oak Ridge show that the Los Alamos studies were quite successful. The ORNL report will provide details of the statistical comparisons of the participant results.

ACKNOWLEDGMENTS

We are grateful to Dr. J. N. P. Lawrence of Los Alamos for his technical support and helpful suggestions in support of the Criticality Dosimetry Program. We are also pleased to acknowledge the sponsorship of the ORNL DOSAR Group for our participation in these experiments. In particular, we acknowledge the support and hospitality afforded us by Howard Dickson, Richard Greene, Walt Gilly, and Robin Denning of ORNL.

REFERENCES

1. J. A. Auxier, Health Phys. 11, 89 (1965).

2. R. L. Long and P. D. O'Brien (Eds.), AEC Symposium Series No. 15, USAEC Rep. CONF-690102.

3. J. W. Poston, J. R. Knight, and G. E. Whitesides, Health Phys. 26, 217 (1974).

4. J. T. Mihalczo, Nucl. Sci, Eng. 16, 291 (1963).

5. D. R. Stone, and J.H. Thorngate, Health Phys. 21, 441 (1971).

6. C. S. Simms, and H. W. Dickson, Health Phys. 37,687 (1979).

7. Private Communication, R. E. Swaja, Oak Ridge National Laboratory, Health and Safety Division, September 18, 1980.

8. D. G. Vasilik and R. W. Martin, The Los Alamos Area and Personnel Neutron and Photon Dosimeters, LAMS Report, to be published (1981).

9. IAEA, Nuclear Accident Dosimetry Systems, IAEA, Vienna, 181 (1970).

10. D. E. Hankins, A Study of Selected Criticality-Dosimetry Methods, LA-3910 (1968).

11. D. F. Petersen, V. E. Mitchell, and W. H. Langham, "Estimation of Fast Neutron Doses in Man by ^{32}S (n,p) ^{32}P Reaction in Body Hair," Health Phys. 6, 1 (1961).

12. D. F. Petersen and W. H. Langham, "Neutron Activation of Sulfur in Hair: Application in a Nuclear Accident Dosimetry Study, Health Phys., 12, 381 (1966).

13. D. E. Hankins, Direct Counting of Hair Samples for ^{32}P Activation," Health Phys. 17, 740 (1969).

14. D. E. Hankins, "Dosimetry of Criticality Accidents Using Activations of the Blood and Hair," Health Phys. 38, 529 (1980).

15. H. Ing and S. Makra, "Compendium of Neutron Spectra in Criticality Accident Dosimetry," Technical Reports Series No. 180, IAEA, Vienna, 1978.

16. C. S. Sims, "Fifteenth Nuclear Accident Dosimetry Intercomparison Study: August 14-22, 1978," ORNL/TM-6554, 1979.

17. J. A. Auxier, W. S. Snyder, and T. D. Jones, "Neutron Interactions and Penetration in Tissue," Chapter 6 of F. H. Attix, and W. C. Roesch (Eds.), "Radiation Dosimetry," 2nd ed., Academic Press, New York, 1968.

18. NRCP (1957), "Protection Against Neutron Radiation up to 30 Million Electron Volts," Natl. Bur. Std. (U.S.), Handbook 63.

19. M. S. Singh, "Kerma Factors for Neutron and Photons with Energies Below 20 MeV," UCRL-52850, 1979.

20. K. Becker, "Solid State Dosimetry," CRC Press, Cleveland, Ohio, 1973.

Printed in the United States of America
Available from
National Technical Information Service
US Department of Commerce
5285 Port Royal Road
Springfield, VA 22161

Microfiche $3.50 (A01)

Page Range	Domestic Price	NTIS Price Code	Page Range	Domestic Price	NTIS Price Code	Page Range	Domestic Price	NTIS Price Code	Page Range	Domestic Price	NTIS Price Code
001-025	$ 5.00	A02	151-175	$11.00	A08	301-325	$17.00	A14	451-475	$23.00	A20
026-050	6.00	A03	176-200	12.00	A09	326-350	18.00	A15	476-500	24.00	A21
051-075	7.00	A04	201-225	13.00	A10	351-375	19.00	A16	501-525	25.00	A22
076-100	8.00	A05	226-250	14.00	A11	376-400	20.00	A17	526-550	26.00	A23
101-125	9.00	A06	251-275	15.00	A12	401-425	21.00	A18	551-575	27.00	A24
126-150	10.00	A07	276-300	16.00	A13	426-450	22.00	A19	576-600	28.00	A25
									601-up	†	A99

†Add $1.00 for each additional 25-page increment or portion thereof from 601 pages up.